PROCEEDINGS OF THE 14TH SYMPOSIUM ON THE GEOLOGY OF THE BAHAMAS AND OTHER CARBONATE REGIONS

Edited by
Fredrick D. Siewers and Jonathan B. Martin

Production Editor:
Fredrick D. Siewers

Gerace Research Centre
San Salvador Island, Bahamas
2010

Front Cover Photograph – "Kelly and the Veggiemorphs" courtesy of Jon Martin

Back Cover Photograph – "Luigi" courtesy of Erin Rothfus

A & A Printing Inc., Tampa, FL

ISBN 0-935909-90-7

THE NORTHERN GUAM VADOSE ZONE: THIRTY YEARS OF W.E.R.I. RESEARCH

Theresa U. Hormillosa
Water and Environmental Research Institute of the Western Pacific, Mangilao, GU

Arne E. Olsen
Department of the Navy, Facilities Engineering Command Southeast, Jacksonville, FL

John W. Jenson
Water and Environmental Research Institute of the Western Pacific, Mangilao, GU

ABSTRACT

The vadose zone of the Northern Guam Lens Aquifer (Lens) is uplifted, eogenetic-limestone that has undergone significant secondary alteration due to dissolution and precipitation of calcium carbonate and fracturing. The complex water flow processes occurring within the vadose zone are unique to uplifted, eogenetic-limestone islands. Over the past thirty years the Water Environmental Research Institute (WERI) has undertaken several studies attempting to quantify the impact of the vadose zone on the temporal and spatial distribution of recharge to the Lens. This research is summarized and related to recently completed field investigations and on-going modeling studies. Data collected during the summer, fall, and winter of 2004-2005 and recharge rates estimated from time series analysis performed on these data is presented. Transfer function models based upon the log-normal distribution and gamma distribution are developed and compared. These time series models show that: 1) mean travel times from the ground surface to the water table are less than two days; 2) the maximum rate of recharge occurs less that one day after a rain storm; and 3) more than 90 percent of recharge from a storm arrives at the water table within one month. These modeling results combined with the results of field investigations and previously conducted research illustrate the unique and complex flow processes occurring within the vadose zone of the Lens and other similar uplifted eogenetic-limestone islands.

INTRODUCTION

The Northern Guam Lens Aquifer (Lens) is the most important source of fresh water for the residents of and visitors to Guam. Currently fresh water production rates range from 130,000 m^3 day^{-1} (Benny Cruz, personal communication, 2006) to 170,000 m^3 day^{-1} (Contractor and Jenson, 2000 and Jocson et al. 2002). This accounts for approximately 80 percent of the total water demand (Contractor and Jenson, 2000 and Jocson et al. 2002). Proposed development by the United States Navy (USN) and United States Air Force (USAF) is expected to place additional demand upon the Lens in the near future. The Lens is a fragile resource that is vulnerable to both salt water contamination from over-exploitation and contamination from surface-applied chemicals and disposal of human and animal waste. Recently the United States Environmental Protection Agency required the Government of Guam, the USN, and the USAF to determine the extent to which the Lens is affected by surface contaminants. The plans for future development and current investigations have focused attention on the vadose zone of the lens; specifically, how the vadose zone affects the quantity and temporal distribution of recharging water from the soil surface to the lens.

Guam is the largest and most southern of the Mariana Islands, located at latitude 13°28' N., longitude 144°45' E (Figure 1). Guam is ap-

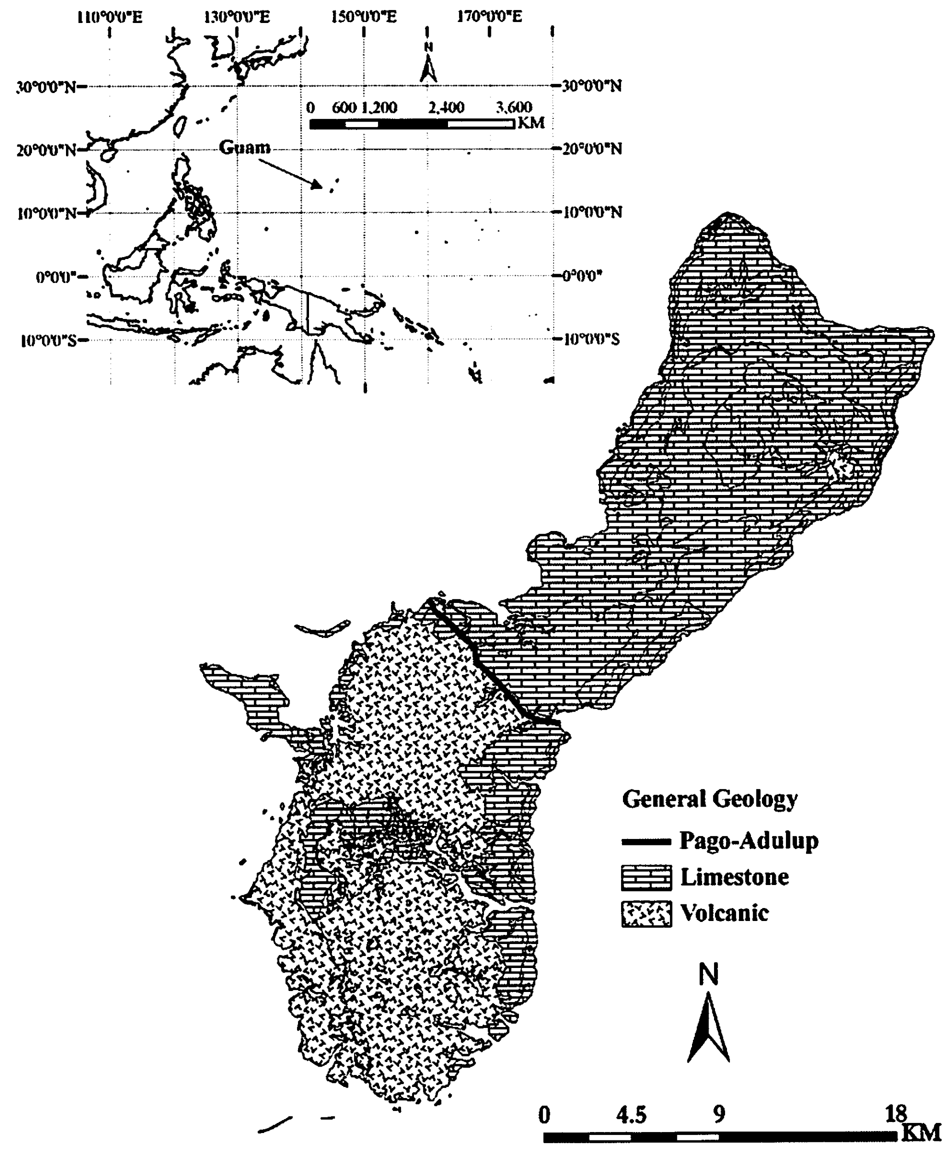

Figure 1. General geology map of Guam, illustrating the relative positions of limestone (north, and south eastern coast) and volcanic rock (the interior south). Additionally, the general location of the Pago-Adulop fault is shown. The map inclusion illustrates the location of Guam within the tropical north western-Pacific.

proximately 48 km long and ranges from 18.5 to 6.4 km wide, with a total area of 550 km^2 (Figure 1). Because of its position in the tropical-west Pacific, Guam receives on average approximately two meters of precipitation annually. The majority of this precipitation arrives during the wet season (July – December). The island is divided into two physiographic provinces of almost equal size (Ward et al., 1965; Mink, 1976; and Mink and Vacher, 1997). The Pago-Adulop Fault separates the southern volcanic highland from the northern limestone plateau (Mink, 1976; Mink and Vacher, 1997). Northern Guam is composed of an undulating limestone plateau (Ward et al., 1965; Mink, 1976; and Mink and Vacher, 1997). This region is characterized by very permeable eogenetic, karst limestone (Mylorie et al., 2001), which includes reef facies ranging from argillaceous lagoonal sediments to massive and compact fore reef assemblages (Mink and Vacher, 1997). The limestones of Northern Guam have been classified as belonging to the late-Miocene Barrigada Limestone, the Plio-Pleistocene Mariana Limestone, and the Holocene Merizo Limestone (Mink and Vacher, 1997; Mylroie et al., 2001).

Hydrogeologically, the most important geological formations are the Barrigada Limestone and the Mariana Limestone (Mink and Vacher, 1997). Both of these have undergone significant fresh water diagenesis that reduces porosity while increasing permeability (Mink and Vacher, 199731-kib1 Mylroie et al., 2001). The process of diagenesis introduces significant vertical and horizontal heterogeneity (Mink and Vacher, 1997; Mylroie et al., 2001) that greatly increases the complexity of flow pathways for both vadose water and ground water. It has been assumed that water flowing through the vadose zone and groundwater of Guam is subject to discrete flow and diffuse flow (Mylroie et al., 1999). Resulting heterogeneity has largely been ignored when studying the flow processes that take place on a basin scale. Generally flow at this scale has been treated using Darcian flow models (Contractor, 1981; Contractor and Srivastava, 1990; Jocson et al., 2002; and Contractor and Jenson, 2000). The Darcian flow theory may not hold at relatively small scales (Jocson et al., 2002).

Early empirical (Mink, 1976) and analytical (Mink, 1976; Mink and Lau, 1977; Ayers, 1981) studies of the Lens addressed neither the temporal distribution of precipitation nor the effect of the vadose zone upon recharge rates. The sustainable yield research conducted by Mink (1976), Mink and Lau (1977), and Ayers (1981) focused on estimating the average annual recharge and the rate at which the recharge water flowed out of the Lens at the coast. These studies are considered to provide a relatively conservative estimate of sustainable yield (Mink, 1991; Jenson and Contractor, 2000; Jocson et al., 2002) and are still used by the Guam Water Authority to manage the groundwater resources of northern Guam. BCG (1992) developed a quasi-analytical model to account for the distinct seasonal pattern of precipitation on Guam. This allowed a significant upward adjustment to the estimates of sustainable yield.

Early numerical modeling of the lens focused primarily on appropriate conceptual and mathematical model development (Contractor, 1981a; Contractor, 1981b; Contractor and Srivastava, 1990). Two more recent numerical investigations of the Lens have focused significant attention on the vadose zone and its impact on the temporal distribution of recharge (Contractor and Jenson, 2000 and Jocson et al., 2002). Jocson et al (2002) developed a model that assumed that all of the recharge that falls as precipitation in one month arrives at the phreatic surface during that month. Their simulations indicated that although some recharge arrived at the lens soon after precipitation, a significant volume travels through the lens at a much slower rate. This observation lead Contractor and Jenson (2000) to develop a vadose zone model that simulated fast, conduit flow and slow, diffuse flow pathways. Their model allowed Contractor and Jenson (2002) to model recharge under different recharge and vadose zone moisture conditions. Based upon a monthly time step, they concluded that approximately one-third of recharge follows the fast, conduit flow pathway and the balance travels through the slow, diffuse flow pathway. Both of these modeling studies (Contractor and Jenson, 2000 and Jocson et al., 2002) assumed that there are distinct rapid and diffuse flow modes.

Two more recent studies by Lander et al. (2001) and Wuerch et al. (2007) shed new light on the timing of recharge. Lander et al. (2001) analyzed the correlation between monthly total precipitation and water table elevation. He determined that, for one well located in the argillaceous member of the Mariana Limestone, water table elevation lags behind precipitation by approximately six months. In the more permeable portions of the Barrigada Limestone and Mariana Limestone the lag was between one and two months. Observations of precipitation and water table elevation at higher temporal resolution show that there is a very rapid response to rainfall. Wuerch et al. (2007) reported that the maximum water table elevation occurred approximately one day after precipitation. Additionally, it has been observed that after heavy precipitation it takes only approximately one month for the water table to return to its original position (Jocson et al., 2002 and Wuerch et al., 2007).

Because of the complex heterogeneity, variety of transport mechanisms, and complex physics of the vadose zone of the Lens, traditional numeric and analytic models may not provide a practical means of assessing recharge mechanism or timing. Relatively recently empirical techniques termed as transfer functions are based on time-series analysis and have been used to assess the flow process occurring in karst vadose zones and aquifers (Padilla and Pulido-Bosch, 1995; Angelini, 1997; Massei et al., 2006; Jukíc and Denic-Jukíc, 2006). Herein we introduce transfer function models for two wells located in the Lens. These models are used to investigate the timing of recharge to the Lens based upon individual recharge events; specifically they determine the time at which the maximum recharge rate occurs, the time when half of the recharge has reached the lens, and the time when 95 percent of recharge has reached the lens.

DATA AND MODELS

Data Description

Meteorological, water table elevation, and salt-fresh water interface data were collected during the summer, fall, and winter of 2004-2005 at four wells located in the Lens. Detailed site description and instrumentation information can be found in Wuerch et al. (2007). Precipitation, water table elevation, and specific conductivity were measured hourly at wells EX-6, EX-7, EX-10, and GHURA from May 24, 2004 until February 28, 2005. Specific conductivity profiles were collected at approximately six-week intervals. Other meteorological data was collected daily by the United States Weather Service at Tiyan, Guam. This investigation will focus on only wells EX-7 and GHURA.

Model Description

One way to assess the degree to which one observed time series may be used to predict another observed times series is the sample cross-correlation function (Padilla, and Pulido-Bosch, 1995; Shumway and Stoffer, 2000). For two time series x_t $(x_1,x_2,x_3,\ldots,x_n)$ and y_t $(y_1,y_2,y_3,\ldots,y_n)$, where x_t causes y_t, and $\overline{x}$, $\overline{y}$ and σ_x, σ_y are the means and variance of the two time series, respectively, the sample cross-correlation function (r_{k+}) is:

$$r_{k+} = r_{xy}(k) = \frac{C_{xy}(k)}{\sqrt{\sigma_x^2 \sigma_y^2}} \tag{1}$$

where

$$C_{xy}(k) = \frac{1}{n}\sum_{t=1}^{n-k}(x_r - \bar{x})(y_r - \bar{y}) \quad (2)$$

Equation 2 defines the sample cross–covariance. This relationship can be expressed in the frequency domain as multiplication of the Fourier transform of the two time series:

$$C_{xy}(f) = X(f) \cdot Y(f)^* \quad (3)$$

where * represents the complex conjugate. Equation 3 can be rewritten in the time domain as:

$$C_{xy}(k) = \int_{-\infty}^{\infty} x(\tau + t)y(\tau)d\tau \quad (4)$$

A relationship similar to equation 3 is the frequency domain transfer function:

$$Y(f) = S(f) \cdot X(f) \quad (5)$$

where S(f) is the travel-time probability density function or impulse response function, which describes how the input time series is mapped into the output time series. This is the convolution of the input series, x_t, with the system function $S(\tau)$ that results in the output series y_t. The relationship can be written as:

$$y_\tau = \int_{-\infty}^{\infty} x(\tau)S(t - \tau)d\tau \quad (6)$$

When the system function S(t) is causal ($Cxy(t) = 0$, $t \leq 0$) the limits of integration may be changed to 0 to ∞. Equation 6 is the definition of a transfer function where the input signal x_t is mapped into the output signal y_t through S(t) the system function (White et al., 1998). This type of model is also termed as the lagged regression model. It assumes that the input signal and the system function are stationary and independent (Shumway and Stoffer, 2000).

Herein the system function is chosen to be either a two parameter log-normal function or a two parameter gamma function. These functions have been selected because: 1) they are causal; 2) their shapes are flexible and therefore represent a large variety of recharge distributions; and 3) their moments can be used to describe temporal recharge characteristics. The two distributions differ in that the two parameter gamma function is less positively skewed and does not have as heavy tails, as compared to log-normal function (Morgan and Henrion, 1990).

It is not feasible to directly measure the amount and timing of water recharging the Lens over a unit area. In order to assess the temporal distribution of water recharging the lens, the surrogate parameters, water table elevation above sea level, and the depth to the salt-fresh water interface were observed. These data are, however, confounded by the net discharge as described by the water balance equation:

$$v\frac{d(h+i)}{dt} = R - D + \varepsilon \quad (7)$$

where η is porosity [-], h is the height of the water table above sea level [m], i [m] is the depth to the salt-fresh water interface [m], t is time [day], R is recharge rate per unit area [m day^{-1}], D is net discharge rate per unit area [m day^{-1}], and ε is the lumped measurement and model error. In order to estimate the depth of the salt-fresh water interface between observations a fourth order polynomial was fit to the data. The recharge rate per unit area will be determined using equation 6 where effective precipitation is the input time series. Effective precipitation is defined as the fraction of total precipitation that leaves the soil layer after accounting for soil water storage and evapotranspiration. A tipping bucket model similar to that used by Bailey et al. (2008) is used to calculate effective recharge. In order to avoid assumptions about the validity of Darcy's Law, a power law:

$$D = ah^b \tag{8}$$

is used to estimate net discharge. Where a [day^{-1}] and b [-] are parameters Equation 8 ensures that net discharge is zero when the water table is at sea level and that, when the parameter b is greater than zero, the net discharge increases as the water table elevation increases.

The parameters of the system functions were determined using an iterative bisection process that minimize the total lumped error term. Two calibration and validation periods were used to develop transfer function models. The calibration periods were June 15, 2004 - July 15, 2004 and October 1, 2004 - October 30, 2004. The validation periods were July 16, 2004 - August 14, 2004 and November 1, 2004 - November 30, 2004. This allowed for the development of linear transfer functions during the relatively wet summer and relatively dry fall.

RESULTS AND DISSCUSSION

Qualitatively, the most obvious feature of the graphs of water table elevation and effective precipitation (Figure 2) is the relatively frequent occurrence of very intense precipitation during the summer followed by a relatively dry fall and winter. This pattern is characteristic of years following El Niño years (Lander et al., 2001). These years also are characterized by a relative abundance of tropical depressions in the general area of Guam. During the 2004 – 2005 study period Wuerch et al. (2008) reported 11 tropical depressions that passed within 350 km of Guam. The most significant in regards to precipitation was Typhoon Tingting that passed north of Guam during late June, and resulted in approximately 0.30 m of rain. Three tropical depressions passed near Guam during a 10 day period during mid-August. The three August storms and Typhoon Tingting resulted in a rapid rise in water table elevation that was soon followed by a rapid decrease in water table elevation. In both cases the water table returned to approximately the same pre-storm elevation within one month following the end of the storm. During the relatively drier fall of 2004 a similar pattern is observed, only at a much smaller scale.

For the summer and fall at wells EX-7 and GHURA, transfer function models were de-

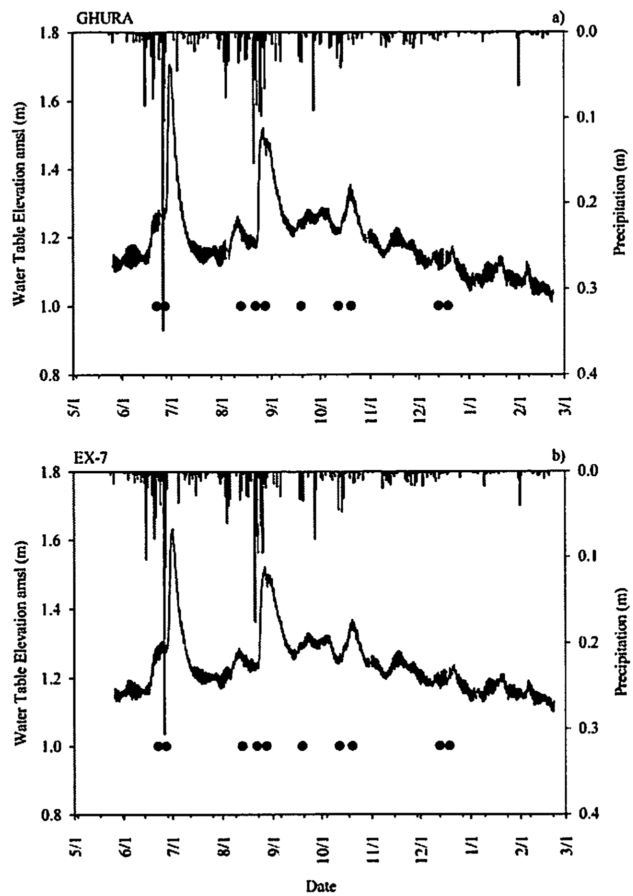

Figure 2. Water table elevation (m) above mean sea level (amsl) for wells a) EX-7 and b) GHURA. Vertical bars are daily precipitation (m). Dots indicate the passage of a tropical cyclone with in 350 km of Guam.

Table 1. Parameters of the transfer function models for wells EX-7 and GHURA during the summer and fall of 2004

Well	Season	Distribution	Mode [day]	Mean [day]	90thPercentile [day]
EX-7	Summer, 2004	Log-Normal	0.47	2.1	4.6
		Gamma	0.63	1.1	2.1
	Fall, 2004	Log-Normal	0.42	2.8	6.3
		Gamma	0.50	2.5	5.5
GHURA	Summer, 2004	Log-Normal	0.44	3.2	7.2
		Gamma	0.81	2.1	4.2
	Fall, 2004	Log-Normal	0.81	5.0	11
		Gamma	1.0	5.0	11

veloped using both the log-normal and gamma distribution. During each period that model was divided into a calibration and validation period. In both seasons, for both distributions, and at both wells the sum-of-squared errors were small as compared to the value of recharge and discharge. The sum-of-squared errors were also similar for both the calibration and validation periods at both wells. These two observations taken together indicate that the recharge transfer models can provide reasonable estimates of recharge. When the summer transfer functions were applied to the fall precipitation data, the sum-of –squared errors increased. The increase in sum-of-squared error was also observed when the fall transfer functions were applied to the summer data.

From the shape of the transfer functions (Figure 3), there is a slight reduction in the average speed at which recharge moves through the vadose in the dryer fall as compared with the wetter summer. Additionally, the length of time that it takes 50 and 90 percent of the effective precipitation (Table 1) to reach the lens in increased. The observations of precipitation and water table elevation data indicate that, during the wet season, precipitation results in a relatively rapid onset of recharge with the majority of recharge arriving at the Lens relatively quickly (Figure 2). These qualitative observations are supported by the quantitative results of the transfer function modeling (Figure 3, Table 1). Both the log-normal and gamma function models for the two periods have maximum rates of recharge occurring in less than one day, with the exception of the gamma distribution at the GHURA well for the fall which has half of the effective precipitation reaching the Lens in less than five days (Table 1). These models also result in 90 percent of all effective precipitation reaching the Lens in less than two weeks. The results of these models stand in contrast to previous studies of the timing of Lens recharge. This is most likely due to the increased temporal resolution of this study.

CONCLUSIONS

The results of this study illustrate that the vadose zone of the Lens transmits the bulk of recharging water very quickly. For both the summer and fall, recharge rates reached a maximum within 48 hours and half of all recharging water reaches the Lens within one week. These results also indicate that a continuous uni-modal travel time probability density function adequately maps effective precipitation into recharge. This is in contrast to previous modeling efforts that have assumed distinct rapid and diffuse recharge modes. The difference between parameters for the summer and fall transfer function indicate that one linear transfer function model is inadequate to model all recharge rates under different vadose zone moisture conditions. More advanced non-linear transfer functions or wavelet transforms may provide a means to estimate recharge rates under different precipitation and vadose zone moisture conditions.

REFERENCES

Angolini, P. 1997. Correlation and spectral analysis of two hydrogeological systems in Central Italy. Hydrological Sciences. 42(3): 425-438.

Ayers, J. F. 1981. Estimates of recharge to the freshwater lens of Northern Guam. Technical Report No. 21. Water and Environmental Research Institute of the Western Pacific, University of Guam, Mangilao. pp. 20.

BCG (Barrett Consulting Group). 1992. Groundwater in northern Guam, sustainable yield and groundwater development. Prepared for the Public Utility Agency of Guam. CDM (Camp, Dresser & McKee, Inc.) 1982: Final Report, Northern Guam Lens Study, Groundwater Management Program, Aquifer Yield Report. Prepared for the Guam Environmental Protection Agency.

Contractor, D. N. 1981a. A one dimensional, finite element salt water intrusion model. Technical Report No. 20. Water and Environmental Research Institute of the Western Pacific, University of Guam, Mangilao. pp. 57.

Contractor, D. N. 1981b. A two dimensional, finite element model of salt water intrusion in groundwater systems. Technical Report No. 26. Water and Environmental Research Institute of the Western Pacific, University of Guam, Mangilao. pp. 47.

Contractor, D. N., and J. W. Jenson. 2000. Simulated effect of vadose infiltration on water levels in the Northern Guam Lens Aquifer. Journal of Hydrology. 229: 232-254.

Contractor, D. N., and R. Srivastava. 1990. Simulation of saltwater intrusion in the Northern Guam Lens using a microcomputer. Journal of Hydrology, 118: 87-106.

Jukíc, D. and v. Deníc-Jukíc. 2006. Nonlinear kernel functions for karst aquifers. Journal of Hydrology. 328: 360-374.

Jocson, J.M.U., J. W. Jenson, and D. N. Contractor. 2002, Recharge and aquifer response: Northern Guam Lens Aquifer, Guam, Mariana Islands. Journal of Hydrology. 260: 231-254.

Lander, M.A. 1994. Meteorological factors associated with drought on Guam. Technical Report No. 75. Water and Environmental Research Institute of the Western Pacific, University of Guam, Mangilao. pp. 39.

Massei, N., J. P. Dupont, B. J. Mahler, B. Laignel, M. Fournier, D. Valdes, S. Ogier. 2005. Investigating transport properties and turgidity dynamics of a karst aquifer using correlations, spectral, and wavelet analyses. Journal of Hydrology. 329: 244-257.

Mink, J. F. 1976. Groundwater resources on Guam: Occurrence and development. Technical Report No. 1. Water and Environmental Research Institute of the Western Pacific, University of Guam, Mangilao. pp. 276

Mink, J. F. and L. S. Lau, 1977. Groundwater analysis by tritium technique: A preliminary evaluation. Technical Report No. 2. Water and Environmental Research Institute of the Western Pacific, University of Guam, Mangilao. pp. 26.

Mink, J. F. and H. L. Vacher. 1997. Hydrogeology of Northern Guam. In: Geology and hydrogeology of carbonate islands. in Developments in Sedimentology 54. Eds. H.L. Vacher and T. Quinn. Elsevier Science. Amsterdam. pp 743-761.

Morgan, M. G. and M. Henrion. 1990. Uncertainty: A guide to dealing with uncertainty in quantitative risk and policy analysis. Cambridge University Press. Cambridge, UK.

Mylroie, J. E., J. W. Jenson, D. Taborosi, J.M.U. Jocson, D. T. Vann and C. Wexel. 2001. Karst Features of Guam in terms of a general model of carbonate island karst. Journal of Cave and Karst Studies. 63(1): 9-22.

Mylroie, J. E., J. W. Jenson, J. M. U. Jocson, and M. A. Lander. 1999. Karst geology and hydrology of Guam: A preliminary report. Technical Report No. 89. Water and Environmental Research Institute of the Western Pacific, University of Guam, Mangilao. pp. 32.

Padilla, A. and A. Pulido-Bosch. 1995. Study of hydrographs of karstic aquifers by means of correlation and cross-spectral analysis. Journal of Hydrology. 168: 73-89.

Shumway, R. H. and D. S. Stoffer. 2000. Time Series Analysis and Its Applications. Springer Scienct+Buiness Media, Inc. New York, NY.

Ward, P. E., S. H. Hoffard, and D. A. Davis. 1965. Hydrology of Guam: Geology and hydrology of Guam, Mariana Islands. Vol. 403-H. U. S. Geological Survey Professional Paper, U. S. Government Printing Office, Washington D. C. pp. 26.

White, R. E., L K. Heng, and R. B. Edis. 1998. Transfer function approaches to modeling solute transport in soils. Iin Physical Nonequilibrium in Soils: Modeling and Applications. Eds. H. M. Selim and L. Ma. Ann Arbor Press, Chelsea, MI. pp. 311-347.

Wuerch, H. V., B. C. Cruz, and A. E. Olsen. 2007 An analysis of the dynamic response of the Northern Guam Lens Aquifer to Sea Level Change and Recharge. Technical Report No. 118. Water and Environmental Research Institute of the Western Pacific, University of Guam, Mangilao. pp. 39.